

# Combustion experiments of liquid kerosene and hydrogen/methane mixing in a dual mode ramjet

*M. Bouchez, MBDA, Bourges, France O. Dessornes, ONERA, Palaiseau, France*

## Nomenclature

$M$	=	Mach number
$\dot{m}_k$	=	Mass flow rate of kerosene (kg/s)
$\dot{m}_{O_2}$	=	Mass flow rate of oxygen (kg/s)
$P$	=	Pressure
$PCI_{CH_4}$	=	Lower heating value of methane (50 MJ/kg)
$PCI_{H_2}$	=	Lower heating value of hydrogen (120 MJ/kg)
$PCI_k$	=	Lower heating value of kerosene (42.9 MJ/kg)
$P_s$	=	Chamber inflow static pressure
$T_i$	=	Stagnation temperature (K)
$\eta_c$	=	Combustion efficiency
$\phi_c$	=	Energetic equivalence ratio

## 1 Introduction

Performed by ONERA and MBDA and supported by the French ministry of defence, the LEA Program,<sup>1</sup> is dedicated to the free flight of a vehicle equipped with a dual mode ramjet, between Mach 4 and 8, in order to check the ground-test and CFD based aeropropulsive design methodology.

Mainly for storage consideration, it was decided to use a hydrogen/methane mixture as fuel. On one hand, the methane allows to reduce the needed tank volume but on the other hand, its ignition characteristics are very poor compared to hydrogen. For this reason, hydrogen is added to enhance the ignition performance. The ignition delay is very sensitive to the percentage of hydrogen in this mixing and studies are needed to investigate the combustion process of such a fuel in supersonic flows. In order to address this problem, fundamental as well as more applied studies have been carried out,<sup>2,3</sup>.

That is why, in parallel with fundamental studies on the combustion of this fuel in supersonic flows, experiments on a known dual mode ramjet developed during the JAPHAR program,<sup>4</sup> have been conducted. Indeed, a complete data base with gaseous hydrogen is available for this engine,<sup>5,6</sup> and those results can be considered as a baseline for comparison with hydrogen/methane fuel. Four percentages of hydrogen in the mixing have been considered as well as four injected equivalence ratios. The flight Mach number simulated for the tests described herein is 7.6 for a dynamic pressure of 0.6 bar.

## 2 Test set-up

### 2.1 ATD 5 test cell

The tests have been performed in the ATD 5 test cell of the Onera centre in Palaiseau, France. This facility has the following capacities :

- $P_i \max \leq 40$  bar,
- $T_i \max \leq 2400$  K
- air mass flow  $\leq 8$  kg/s
- $O_2$  mass flow  $\leq 1.4$  kg/s
- $H_2$  mass flow  $\leq 0.3$  kg/s

For the maximum temperature, the flow rate is limited to around 4 kg/s. The air is pre-heated thanks to a air/ $H_2$  combustion with molar oxygen replenishment.

### 2.2 Test chamber geometry

The studied dual mode ramjet concept was developed in the frame of the JAPHAR project. This engine was supposed to be able to power an experimental vehicle in order to assess the propulsive balance of a dual mode ramjet. On the basis of

PREPHA's previous work, this hydrogen fuelled dual mode ramjet has been designed for large engines,<sup>7</sup> and consequently, struts are used to inject the fuel (fig. 1).

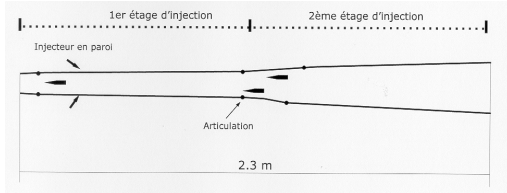


**Figure 1. Experimental chamber**

The upstream part of the chamber is slightly diverging and is essentially devoted to supersonic combustion whereas the second part which has greater divergence angles allows to work in subsonic or in transitional regime (fig. 1). The geometry has been defined to be completely supersonic at Mach 8 when the whole hydrogen is injected in the first chamber part.

The transition between the two combustion modes, subsonic-supersonic, is controlled thanks to the injection repartition between the two injection levels. For the subsonic regime a thermal throat is used rather than a mechanical throat that should be removed for the supersonic combustion regime.

Taking into account the capacities of the ONERA's test facility, an experimental engine has been designed. The chamber entrance cross section is  $100 \times 100 \text{ mm}^2$  and the engine is 2.3 meters long. The first injection stage has only one strut and wall injections are added in order to simulate a row of struts. The second injection stage is constituted by two struts.

The test set-up in ATD 5 test cell is shown fig.2. For the injection system, cooled struts made of copper have been used (fig. 3). These struts are directly inspired from previous PREPHA work,<sup>8</sup>. They have eight lateral injections and 3 base injections.

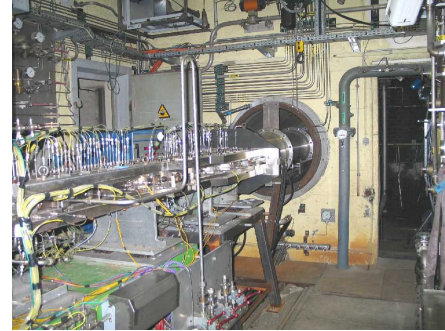


**Figure 2. Test set up**

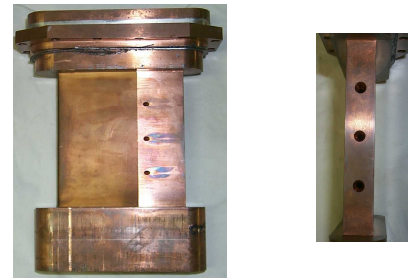


**Figure 3. Injection strut**

The two upstream wall injections are constituted each by three supersonic nozzles inclined at  $45^\circ$  in the stream direction. This angle which gives a good compromise between the jet penetration and the conservation of the jet momentum was also adopted for the injectors the struts walls,<sup>8,9,10,11</sup>.

To enhance the mixing at the strut base, Glawe and all. have shown that the exit Mach number of the base nozzles should be kept above the Mach number of the main flow at the base,<sup>12</sup>. For this reason the Mach number of base injectors is set to 2.8.

For these tests performed for Mach 7.6 flight conditions, the second injection level was removed.

## 2.2 Calorimeter

To determine the combustion efficiency, a calorimeter was used. This device principle is to freeze the combustion gases at the end of the chamber by injecting water and then to measure the mean temperature of the mixing at the exit of the calorimeter. Then, the amount of burnt fuel and the combustion efficiency are determined with a simple

heat balance (Eq. 1). The unknowns are  $T_{gi}$  and the gas composition. A thermochemistry code is used in an iterative process to determine these values.

$$\int_{T_{ce}}^{T_{gi}} C_p dT = m_w [C_{p_{lw}}(373 - T_{w_i}) + Lv + C_{p_{gw}}(T_{ce} - 273)] + Q_i \quad (1)$$

In our experiment, the water is injected at 1 bar and boils at 373 K. The heat capacity of the water steam is supposed to be constant in our range of temperature (between 400 and 800 K). The minimum temperature at the exit of the calorimeter is around 400 K to ensure that the water is vaporized. In addition, at the exit of the calorimeter, the temperature homogeneity is verified with several thermocouples. This device has been previously assessed during tests performed with a classical ramjet.

### 3 Test conditions

For the inflow, the Mach number, static pressure and static temperature are the same as compared to the vehicle trajectory at  $P_{dyn} = 0.6$  bar. The inflow conditions for the different flight Mach numbers are as follows :

$M_\infty$	$M_i$	$P_{i1}$ (bar)	$T_{i1}$ (K)	$P_1$ (Pa)	$T_1$ (K)
7.6	3.11	29.0	2470	51450	1135

**Table 1. Test conditions**

The air that is pre-heated thanks to air/ $H_2$  combustion has the following mass fraction compositions :

$M_\infty$	$O_2$	$N_2$	$H_2O$
7.6	0.280	0.414	0.306

**Table 2. Inflow gas composition**

Four equivalence ratios were investigated : 0.3, 0.5, 0.7 and 1.0. The tests lasted 6 seconds in steady conditions. Two different fuels, hydrogen/methane mixing and liquid kerosene were used.

For the hydrogen/methane mixing, four mass percentages of hydrogen were tested between 5 and 30%, and refereed as  $A\% < B\% < C\% < D\%$ . As the

heating value of these mixing varies from one to another the comparison between the results was made on the basis of an “energetic equivalence ratio” defined as the equivalent amount of kerosene needed to obtain the same heat release (eq. 2).

$$\varphi_e = \frac{3.421(mk_1 + mk_2)}{mO_2} \text{ with } mk_1 = \frac{PCI_{H_2}}{PCI_k} mH_2$$

$$\text{and } mk_2 = \frac{PCI_{CH_4}}{PCI_k} mCH_4 \quad (2)$$

$mO_2$  corresponds to the remaining flow rate of oxygen contained in the air after it was pre-heated through the hydrogen/air burner and also after oxygen molar replenishment.

### 4 Test results

The principal obtained results are pressure profiles along the test chamber, heat flux on the walls and combustion efficiencies. From the obtained pressure profiles, 1D inverse analysis were made thanks to the PUMA code developed by MBDA. First of all, it should be mentioned that the self-ignition of the mixing was always obtained within the mass percentage of hydrogen dealt with.

The two following figures show the obtained pressure profiles for an energetic equivalence ratio of 1 and for the four tested different percentage of hydrogen in the hydrogen/methane mixing. It can be seen that there seem to be two different types of heat distribution in the chamber that give more or less two types of pressure distributions along the chamber.

For the lower percentage of hydrogen, the pressure profile rise happens further in the test chamber than for higher percentages (C and D) which is particularly true for the right wall (Fig. 5). Then, for these low hydrogen percentages (A and B) comes a strong pressure rise located near 900 mm in abscissa. This could indicate that the ignition delay of the mixing is slower than for higher percentage. The burning of the hydrogen which begins very rapidly could provide not enough heat release to dramatically enhance the

burning of methane. On the contrary, when the ignition conditions are met for methane, a large heat release is suddenly provided which gives the pressure rise at 900 mm.

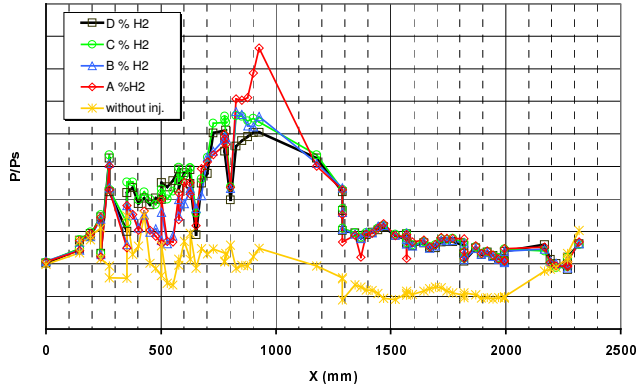


Figure 4. Pressure profiles for the upper wall ( $\phi_e = 1$ )

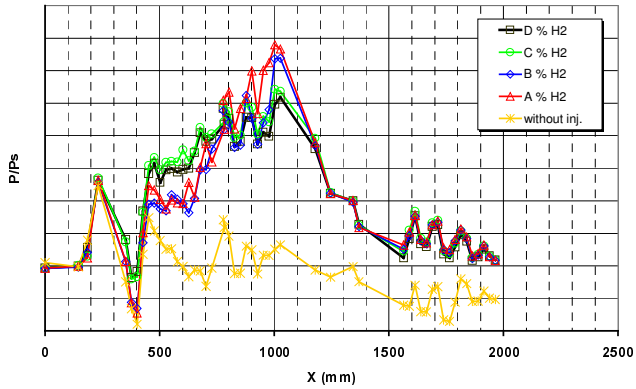


Figure 5. Pressure profiles for the right wall ( $\phi_e = 1$ )

For the highest percentages of hydrogen tested, the heat release along the chamber seems to be more smoothly distributed which leads to a better distribution of the fuel consumption along the chamber and to smoother pressure profiles as well.

At the end of the chamber, the pressure levels attained are very similar and the different pressure curves are nearly the same. This indicates that most of the combustion has ended before the last third of the chamber, namely before  $X = 1200$  mm. However, this does not mean that the combustion efficiencies are exactly the same since one particular pressure profile

depends on the heat released, the heat losses through the wall and also on the pressure losses. This will be discussed further.

The pressure profiles obtained for different equivalence ratios and case C of  $H_2$  are shown Fig. 6 and Fig.7. As waited, the greater the equivalence ratio the greater the pressure. On the right walls, the shock emanating from the leading edge of the struts is clearly reflected on the walls. This is particularly visible up to  $\phi_e = 0.7$  until  $X = 700$  mm. For  $\phi_e = 1$ , the combustion process begins very rapidly which leads to a pressure rise just after the injection strut (around  $X = 500$  mm) and the shock reflections are no longer visible. Moreover, the ignition length clearly decreases with increasing equivalence ratio.

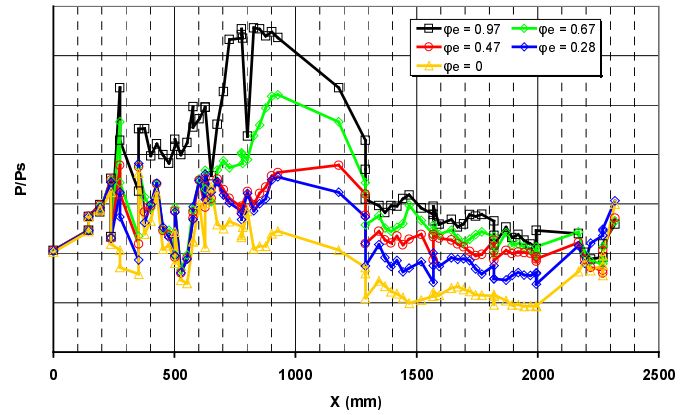


Figure 6. Pressure profile for C% of  $H_2$ , upper wall.

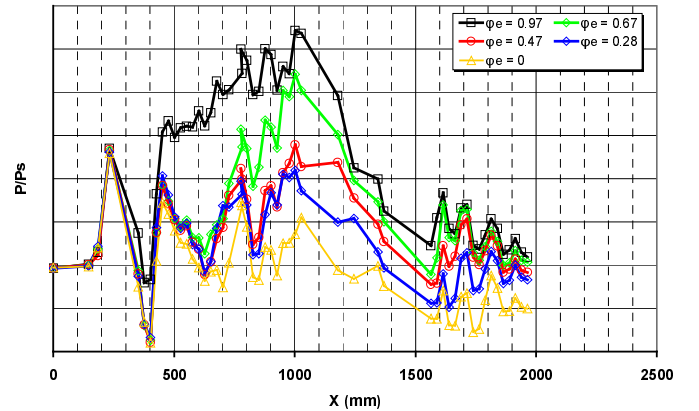


Figure 7. Pressure profile for case C, right wall.

It leads fact that the pressure profiles keep longer the same at the lowest equivalence ratios. For

example, the discrepancy between  $\phi_e = 0.5$  and 0.3 appears only after 1 meter while it appears much sooner between  $\phi_e = 0.7$  and 0.5 ( $X = 700$  mm).

When compared to the profile without injection, the ignition length can be estimated between 150 mm behind the strut for  $\phi_e = 1.0$  to 500 mm for  $\phi_e = 0.3$ .

The figure 8 shows the heat flux densities measured along the walls for the different tested equivalence ratios and C % of  $H_2$ . The equivalence ratio influence is very clear with increasing heat flux values for increasing  $\phi_e$ . In particular, the heat flux in the first part of the chamber ( $X = 800$  mm) reaches 3.8 MW/m<sup>2</sup> for  $\phi_e = 1.0$  and hardly attains 1.7 MW/m<sup>2</sup> for  $\phi_e = 0.3$  or 0.5. This indicates again that the combustion began very rapidly behind the injections for  $\phi_e = 1.0$  whereas it was delayed for 0.3 and 0.5. At the end of the chamber, the differences between the curves decrease. Nonetheless, the ratio between the greatest and the lowest value of 2 keeps significant. The high values of heat flux attained also point out the fact that this is probably an issue to diminish them since they are pure losses for the propulsion purpose.

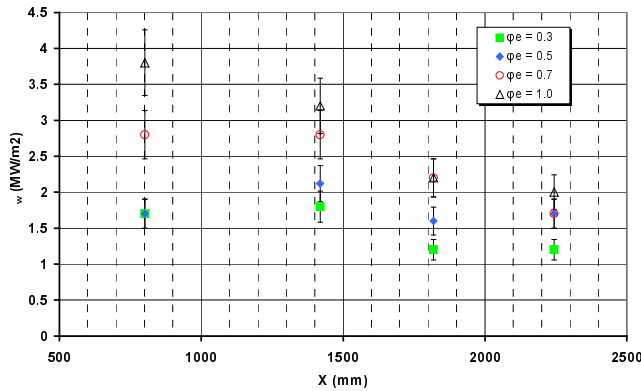


Figure 8. Heat flux density for case C versus X

Concerning the combustion efficiencies, the results are summarized Fig. 9. Those results were obtained with the calorimeter assuming losses through the walls deduced from the heat flux gages. For this comparison, the results obtained with pure kerosene are also included. First of all, the best results were obtained with kerosene. This probably comes from the fact that the ignition is not really a problem for Mach 7.6 flight conditions. In addition, the jet penetration and fuel distribution in the chamber is probably better

with an atomized liquid jet than with pure gas. As a consequence, kerosene gives here good results which certainly wouldn't be the case for lower Mach numbers. For the different hydrogen contents in the injected gaseous mixture, it can be seen that the best results were obtained for case C of hydrogen percentage.

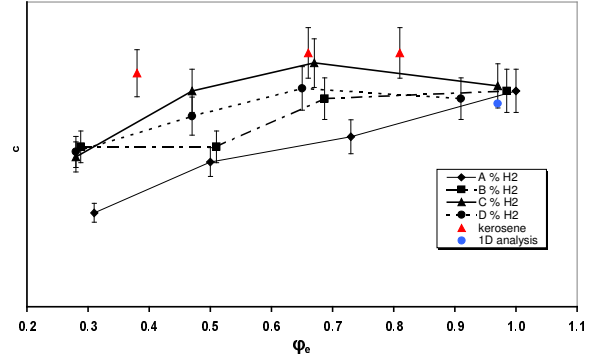


Figure 9. Combustion efficiencies

However, due to the error that may occur when computing the efficiency due to the wall heat losses estimates, one can say that the results between C and D of % $H_2$  are nearly the same. Even the results for B are not so far from the two previous results and only the efficiencies for case A (lower % of  $H_2$  here) are quite lower than the others. The tendency is an increase in the efficiency with increasing  $H_2$  content. However, an increase in the hydrogen percentage leads to a injection jet momentum decrease since the density decreases. As a result, the jet penetration becomes lower and the mixing becomes probably poorer. Eventually, there may coexist two contradictory effects when the hydrogen percentage is increased. On one hand, the ignition becomes faster and easier but on the other hand the mixing and the fuel distribution could be less favorable. As a consequence, there could exist a trade off between those to effects that would lead not to increase too much the hydrogen percentage.

Finally, 1D inverse computations were made using the PUMA code developed by MBDA. The principle of this computation is to fit the pressure curve by adjusting the heat release law along the test chamber. In this code, the friction coefficient are adjusted according to the no-reacting case. The wall temperature is set to a measured value and the heat

losses on the walls are computed and taken into account for the resulting pressure profile.

The following computed results are given for case C and  $\phi_e = 1.0$ . The figure 10 shows the experimental pressure profile and the fitted 1D pressure profile. The Mach number evolution is shown Fig. 11. The flow remains supersonic all the chamber long.

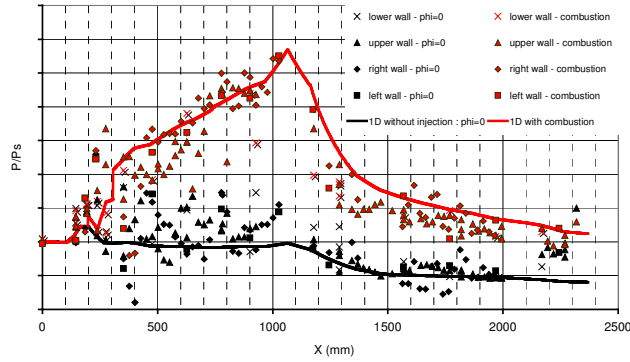


**Figure 10. 1D computed and experimental pressure profile**

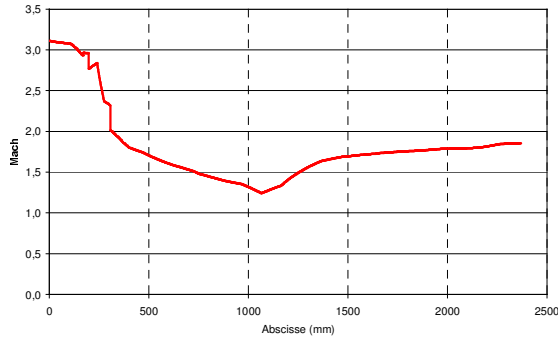


**Figure 11. 1D computed Mach number**

The flow is decelerated in the first part of the chamber and the Mach number reaches roughly 1.2 at the end of this part. Then, due to the diverging angles, the flow reaccelerates in the second part of the chamber and reaches finally Mach 1.9.

The combustion efficiency evolution is shown Fig. 12. Between 70 % to 80% of the final combustion efficiency is achieved within the first meter. Then, more than one other meter is needed to obtain the final level. This is consistent with previous results obtained with pure hydrogen. As this engine was designed to

work from Mach 4 to 8 with a fixed geometry, the second part of the chamber which is mostly dedicated to subsonic combustion has large diverging angles that are not suited to pure supersonic combustion. However, this is not detrimental to this concept since the second part is mandatory for the subsonic combustion mode for this design.

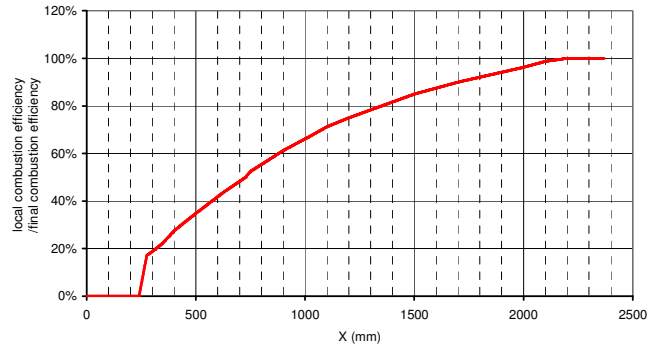


**Figure 12. 1D computed combustion efficiency evolution**

## 5 Conclusion

Within the LEA program, the aim of this study was to have first experimental data on the combustion of hydrogen/methane mixing. Tests were performed for Mach 7.6 conditions in a well known combustion chamber used previously for the JAPHAR program. Four hydrogen mass percentages between 5 and 30% were tested for energetic equivalence ratios between 0.3 and 1.0. The self-ignition was always obtained for these conditions. However, a sensitivity to the percentage of hydrogen was found and the best results were obtained for the higher percentages of hydrogen in the mixing. In parallel, tests with liquid kerosene were also performed and showed better performances due to a better fuel repartition in the chamber. However, this is probably a particular case and for lower flight Mach numbers, the ignition of kerosene could be questionable.

To continue the study, a new test chamber called CLEA is currently designed to meet the LEA

requirements in terms of chamber length, height and width. This test chamber will be heavily tested with the hydrogen/methane fuel mixing on and after 2006.

## References

<sup>1</sup>F.Falempin, "LEA flight test program Status in 2004", IAC-04-S.5.02, 55th International Astronautical Congress of the International Astronautical Federation, the International Academy of Astronautics, and the International Institute of Space Law, Vancouver, Canada, Oct. 4-8, 2004

<sup>2</sup>D. Davidenko, I. Gökalp, E. Dufour, D. Gaffié, « *Kinetic mechanism validation and numerical simulation of supersonic combustion of methane-hydrogen fuel* », AIAA paper 2002-5207, 11<sup>th</sup> AIAA/AAAF International conference on space planes and hypersonic systems and technologies, 29 septembre – 4 octobre 2002, Orléans, France.

<sup>3</sup>V. Quintilla, P. Magre, and D. Scherrer, P. Destors, E. Dufour, " *Experimental and Numerical Investigation of Supersonic Reacting Hydrogen/Methane Jets in Hot Air Co-Flows*", AIAA-2005-3301, AIAA/CIRA 13th International Space Planes and Hypersonics Systems and Technologies Conference

<sup>4</sup>P. Novelli, W. Koschel, " *JAPHAR – A joint ONERA-DLR research project on high speed airbreathing propulsion*", ISABE paper 99-7091, 14<sup>th</sup> Symposium ISABE, Florence (Italy), September 05-10, 1999.

<sup>5</sup>O. Dessornes, D. Scherrer, " *Tests of the JAPHAR dual mode ramjet engine*", AST 9 (2005) p211-221

<sup>6</sup>O.Dessornes, Scherrer D., Novelli P., " *Testing and weighing of the japhar dual mode ramjet engine*", ISABE paper 2001-1135, Bangalore (India).

<sup>7</sup>F. Falempin, H. Lacaze, A. Wagner, P. Viala, " *Reference and generic vehicle for the French hypersonic technology program*", AIAA paper 95-6008, AIAA 6th international aerospace planes and hypersonics technologies conference, Chatanooga (USA) 1995

<sup>8</sup>O. Dessornes, C. Jourden, " *Mixing enhancement techniques in a scramjet* ", 8<sup>th</sup> AIAA International space planes and hypersonic systems and technologies conference, Norfolk (USA), April 27-30, 1998

<sup>9</sup>Povinelli F., Povinelli L. A., Hersch M., " *Supersonic jet penetration (up to Mach 4) into a Mach 2 Airstream*", AIAA paper 70-92, 1970

<sup>10</sup>M. Gruber, A. Nejad, J. Dutton, " *An experimental investigation of transverse injection from circular and elliptical nozzles into a supersonic crossflow*", Wright laboratory final report, January 1996, WL-TR-2102

<sup>11</sup>D. Bayley, R. Hartfield, " *Experimental investigation of angled injection in a compressible flow*", AIAA paper 95-2414, July 1995

<sup>12</sup>Glawe D., Samimy M., Nejad A., " *Nozzle geometry effects on strut injection into a supersonic flow*", Wright laboratory final report, September 1995, WL-TR-95-2143